NASA/TM–2015-218970

Fiber Optic Rosette Strain Gauge Development and Application on a Large-Scale Composite Structure

Jason P. Moore, Adam Przekop, and Peter D. Juarez
Langley Research Center, Hampton, Virginia

Mark C. Roth
Modern Machine and Tool Company, Inc., Newport News, Virginia

December 2015

NASA STI Program . . . in Profile

Since its founding, NASA has been dedicated to the advancement of aeronautics and space science. The NASA scientific and technical information (STI) program plays a key part in helping NASA maintain this important role.

The NASA STI program operates under the auspices of the Agency Chief Information Officer. It collects, organizes, provides for archiving, and disseminates NASA's STI. The NASA STI program provides access to the NTRS Registered and its public interface, the NASA Technical Reports Server, thus providing one of the largest collections of aeronautical and space science STI in the world. Results are published in both non-NASA channels and by NASA in the NASA STI Report Series, which includes the following report types:

- TECHNICAL PUBLICATION. Reports of completed research or a major significant phase of research that present the results of NASA Programs and include extensive data or theoretical analysis. Includes compilations of significant scientific and technical data and information deemed to be of continuing reference value. NASA counter-part of peer-reviewed formal professional papers but has less stringent limitations on manuscript length and extent of graphic presentations.

- TECHNICAL MEMORANDUM. Scientific and technical findings that are preliminary or of specialized interest, e.g., quick release reports, working papers, and bibliographies that contain minimal annotation. Does not contain extensive analysis.

- CONTRACTOR REPORT. Scientific and technical findings by NASA-sponsored contractors and grantees.

- CONFERENCE PUBLICATION. Collected papers from scientific and technical conferences, symposia, seminars, or other meetings sponsored or co-sponsored by NASA.

- SPECIAL PUBLICATION. Scientific, technical, or historical information from NASA programs, projects, and missions, often concerned with subjects having substantial public interest.

- TECHNICAL TRANSLATION. English-language translations of foreign scientific and technical material pertinent to NASA's mission.

Specialized services also include organizing and publishing research results, distributing specialized research announcements and feeds, providing information desk and personal search support, and enabling data exchange services.

For more information about the NASA STI program, see the following:

- Access the NASA STI program home page at http://www.sti.nasa.gov

- E-mail your question to help@sti.nasa.gov

- Phone the NASA STI Information Desk at 757-864-9658

- Write to:
  NASA STI Information Desk
  Mail Stop 148
  NASA Langley Research Center
  Hampton, VA 23681-2199

NASA/TM–2015-218970

Fiber Optic Rosette Strain Gauge Development and Application on a Large-Scale Composite Structure

Jason P. Moore, Adam Przekop, and Peter D. Juarez
Langley Research Center, Hampton, Virginia

Mark C. Roth
Modern Machine and Tool Company, Inc., Newport News, Virginia

National Aeronautics and
Space Administration

Langley Research Center
Hampton, Virginia 23681-2199

December 2015

Available from:

NASA STI Program / Mail Stop 148
NASA Langley Research Center
Hampton, VA 23681-2199
Fax: 757-864-6500

Introduction

NASA's Environmentally Responsible Aviation Project was created to explore and document the feasibility, benefits, and technical risk of advanced vehicle configurations and enabling technologies that will reduce the impact of aviation on the environment [1]. One such enabling technology is Pultruded Rod Stitched Efficient Unitized Structure (PRSEUS), which is a new lightweight composite structure design incorporating integrally stiffened panels that are stitched together and configured to maintain residual load-carrying capabilities under a variety of damage scenarios. As a culmination of a joint effort between NASA and The Boeing Corporation to investigate the feasibility of incorporating new technologies such as PRSEUS into the design of next generation unconventional aircraft, a large-scale (30 x 14 x 7 ft^3 w-h-d) multi-bay fuselage test article incorporating PRSEUS technology was designed and constructed. The design of the test article focused on meeting weight and strength goals established for a Hybrid Wing Body (HWB) concept vehicle and is an 80%-scale representation of the center section of an HWB aircraft pressure cabin (figure 1). The test article was subjected to load and pressure tests in NASA Langley Research Center's Combined Loads Test System (COLTS) in the pristine state and an impact-damaged state. The structural monitoring systems used to monitor the behavior of the test article during testing included resistive strain gauges, acoustic emission (AE) sensors, video image correlation (VIC) systems, fiber optic (FO) strain gauges, and linear variable differential transducer (LVDT) displacement sensors. The FO strain gauge suite consisted of the traditional linear, single-axis distributed strain gauge arrangement and a newly developed FO rosette-style, multi-axis strain gauge arrangement. What follows is a detailed description of the construction, application, and measurement of 196 FO rosette strain gauges that measured multi-axis strain across the outside upper surface of the forward bulkhead component of the multi-bay fuselage test article. A background of the FO strain gauge and the FO measurement system as utilized in this application is given and results for the higher load cases of the testing sequence are shown.

Figure 1: photograph of the large-scale multi-bay fuselage test article in a holding fixture

Background: Fiber Optic Strain Sensors and Interrogators

A fiber Bragg grating (FBG) is a section of optical fiber in which the core has been manipulated to have a periodically modulated refractive index [2, pp 1-2]. Illustrated in figure 2, this periodic refractive index modulation creates a resonance reflection condition, known as the Bragg condition, at a wavelength, λ_B, that is equal to twice the physical length of the index modulation, Λ, multiplied by the effective refractive index, n_{eff}, of the fiber core in the FBG region. If a broadband light source is coupled into optical fiber FBG region, light that is not of the Bragg wavelength passes through the FBG region while light at the Bragg wavelength is reflected.

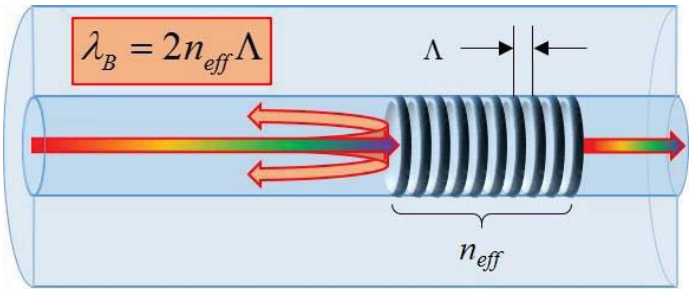

Figure 2: a fiber Bragg grating

Because the Bragg wavelength is directly proportional to the physical spacing of the index modulation in the FBG, any lengthening or shortening of the FBG region of the optical fiber is measureable by tracking the Bragg wavelength of the FBG. By tracking the Bragg wavelength, strain in the FBG region can be found using

$$\varepsilon = \frac{\Delta\lambda_B}{\lambda_B\left(1 - p_e\right)}, \tag{1}$$

where $\Delta\lambda_B$ is the measured change in Bragg wavelength as a result of an externally induced strain, ε, that shifts the Bragg wavelength from the zero-strain value, λ_B, and p_e is the effective strain-optic constant of the optical fiber [2, p 98].

The FBGs used in the application discussed here were constructed by "writing" several hundred weakly-reflecting FBGs into optical fiber as it is was manufactured. In this method, the output of a UV laser is split and recombined through a phase mask before being incident on the fiber between the stages of furnace draw and permanent coating application. Because the optical fiber core is slightly reactive to UV energy and because the incident light has a periodically modulated beam cross section (as a result of the phase mask split/recombine), FBGs are implanted into the core during the drawing of the fiber. The result is a strong, reliable, sensing fiber that can be bonded to a surface of interest to provide for hundreds of surface strain measurements throughout the length of the fiber. The fiber optic sensing cable used in this application was part number DTG-LBL-15550AGF, commonly referred to as "all-grating-fiber", from FBGS Technologies GmbH. It is single mode fiber with 125 µm cladding diameter, ORMOCER® (acrylate) coated to 195 µm typical diameter, with a 6 µm mode field diameter @1550 nm. The embedded FBG sensors are low reflectivity (<0.1%) having a 1550 nm nominal Bragg wavelength, a length of 9 mm, and a continuous 10 mm center-to-center distribution.

To interrogate and ultimately track the Bragg reflection of hundreds of weakly-reflecting FBGs spatially distributed in a single sensing fiber, an optical frequency domain reflectometer (OFDR) is used. Illustrated in figure 3, an OFDR interrogator relies on a highly-coherent, mode-hop free, swept laser to create an

interference pattern in a Michelson interferometer consisting of the reflected light of the sensing fiber and the reflected light from a broadband reflector[3, pp 426-429]. As the laser is swept, the interference pattern is detected, amplified, and sampled. The sampled pattern is Fourier transformed and processed to reveal the Bragg wavelength of every FBG in the sensing fiber.

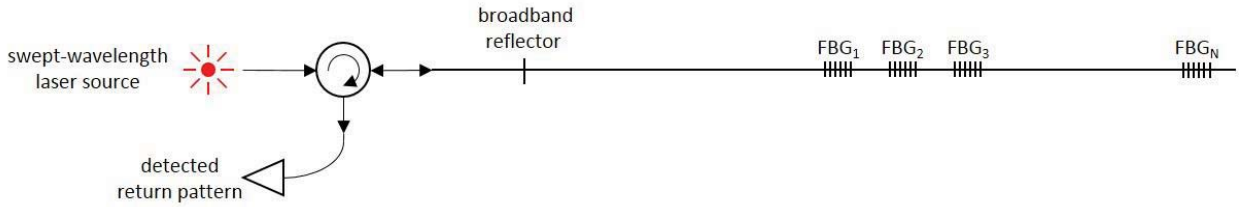

Figure 3: simpified OFDR configuration

The OFDR interrogator used to collect data in this application was a RTS150 manufactured by 4DSP LLC. It was configured to measure strain at 0.5" intervals along four separate sensing fibers of maximum length 42.7 feet simultaneously at approximately 23 Hz. Of note is that the RTS150 interrogator is not configured to measure the Bragg wavelength of each individual FBG sensor in the sensing fiber. Alternatively, it is configured to track the Bragg wavelength of 1024 consecutive 0.5" sections of sensing fiber making up the 42.7 feet of sensing length, irrespective of the exact location of individual FBGs. Because the sensing fiber used in this application is filled with FBGs 9 mm in length with a 10 mm center-to-center spacing, any arbitrary 0.5" section of sensing fiber contained at least a 0.46" length of FBG region within it.

Background: Distributed Fiber Optic Rosette Layout Specification

Figure 4 shows the location specification for the distributed FO rosette locations on the forward bulkhead of the test article. The approximate span length of the bulkhead was 26 feet and the center-point of the rosette gauges were to be located 2.59 in. below the bottom edge of the bulkhead-crown flange.

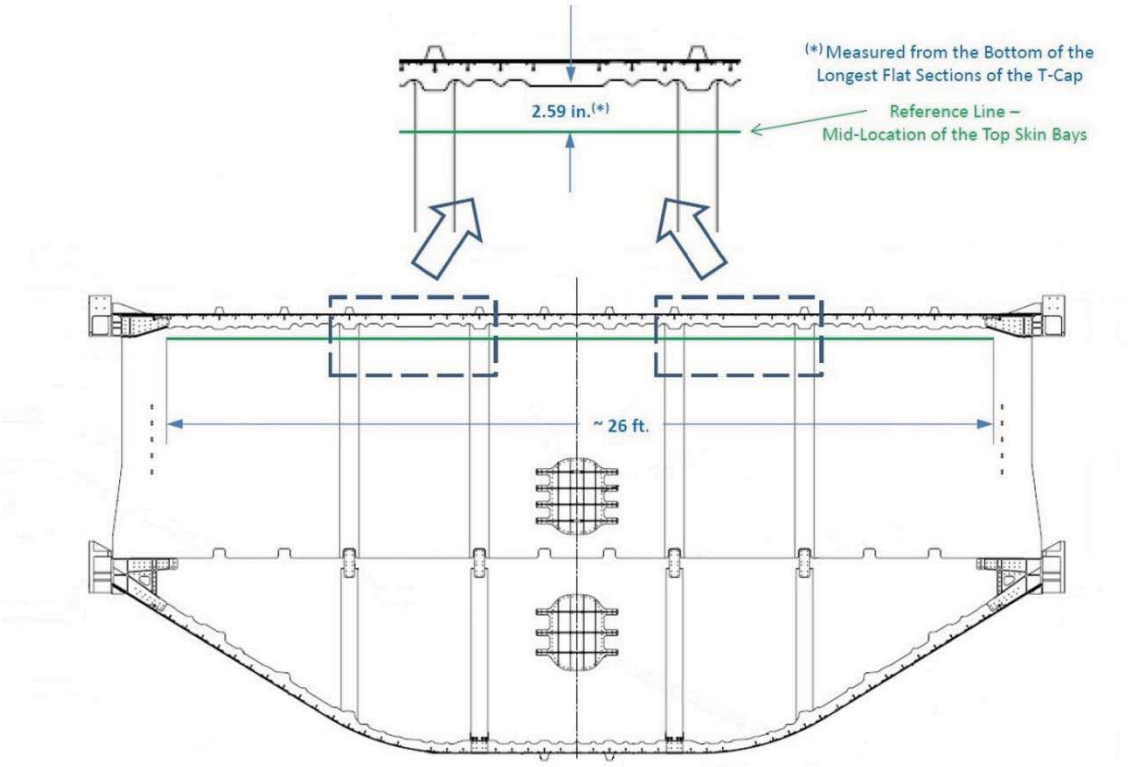

Figure 4: forward bulkhead fiber optic rosette location specification

Figure 5 shows a detailed layout specification for the FO rosettes. Two fibers were to be used to create consecutively arranged 60°-delta rosette gauges with 1.5" side lengths.

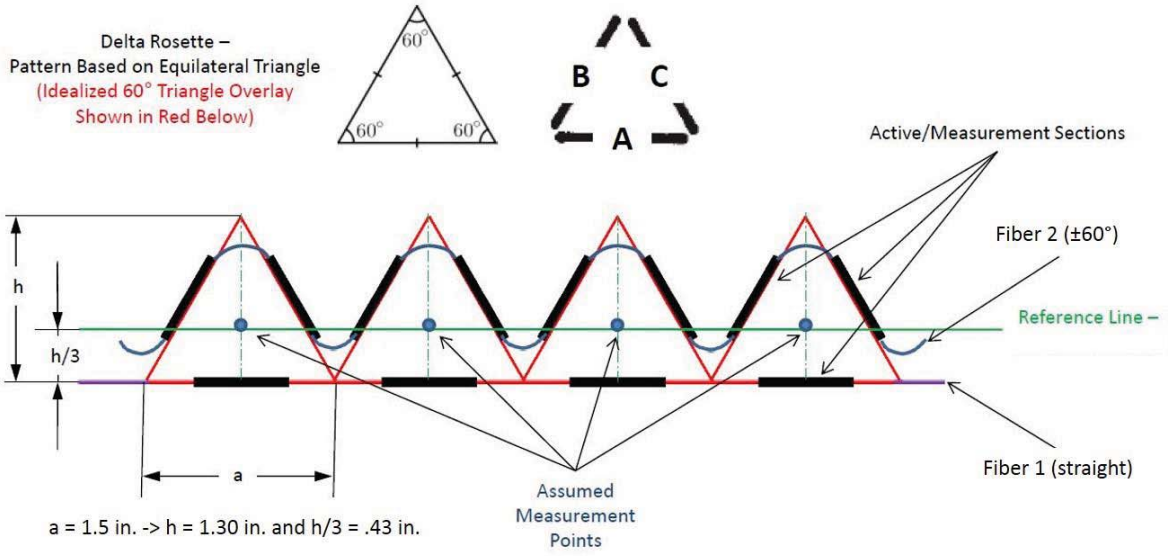

Figure 5: fiber optic rosette layout specification

With an approximate span of 26 feet and a gauge length of 1.5", up to 208 FO rosette gauges were called for in the specification. Due to the anticipated difficulty in configuring FO sensing cable accurately into so many consecutive FO rosette formations directly to the test surface, the application of the FO sensing cable

onto the test article in the form of FO rosette strain gauges was accomplished via two separate procedures. First, separated from the test article, the FO rosettes were configured and spot-bonded to a fiber glass mesh substrate according to the layout specification. The resulting substrate/fiber combination was then laid out onto the test article and bonded according to the location specification.

Fiber Optic Rosette Construction

The mesh substrate was common drywall joint tape, specifically USG VALUEMESH™ joint tape. It was 1 7/8" wide fiberglass-filament mesh with a 1/8" grid pattern and a light-duty adhesive applied to one side. The UV-curable cement used to spot bond the FO sensing cable to the mesh substrate was part number U307 from Cyberbond LLC. It is a medium-to-high viscosity adhesive with a <6 sec. setting time. Prior to rosette construction, the mesh substrate was wholly unspooled and taped to the test article for the purpose of determining exactly where and how many FO rosette gauges would be located on the mesh. Four fasteners approximately 0.375" in diameter were found to be protruding from the test surface in such a way as to interfere with an absolutely continuous distribution of FO rosette gauges across the entirety of the bulkhead span. To accommodate these areas, it was decided that the layout of the FO cable at the fastener locations would deviate from the rosette configuration and be routed in such a way as to by-pass the fasteners and subsequently resume rosette configuration. To insure that the mesh/fiber construct would lay flush to the test surface unimpeded by the protruding fasteners, just enough material was removed from the mesh as to allow it to lay flush around the fasteners. Cable egress and fastener protrusion ultimately led to the following FO rosette layout plan: the mesh substrate would hold three groups of consecutive FO rosettes; the first group was to contain 60 rosettes, the second group 76 rosettes, and the third group 60 rosettes, for a total of 196 FO rosettes. Between the first and second group and between the second and third group would be a three inch section of substrate on which the fibers were positioned to run between fasteners protruding from the surface of the test article. The desired location of each FO rosette on the mesh was labelled using red marker. The mesh substrate was then removed from the test article and neatly spooled.

To accurately position the FO strain sensing cables onto the mesh substrate in the desired rosette pattern, a lay-out pattern was constructed using SolidWorks CAD software. The lay-out pattern drawing is shown in *appendix a* and a portion of it is shown in figure 6.

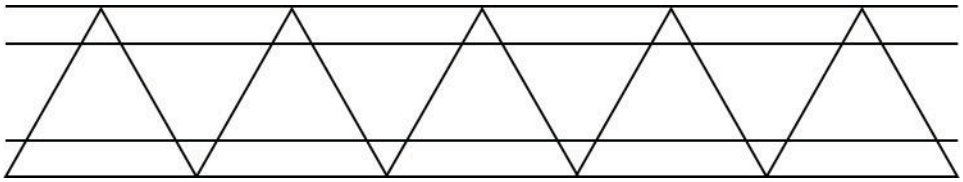

Figure 6: fiber layout template

Illustrated in figure 7, the layout pattern was secured to a working surface using semi-transparent Teflon tape for the purpose of positioning sections of the mesh substrate over it at which point the FO sensing cables could be routed and secured properly to the mesh.

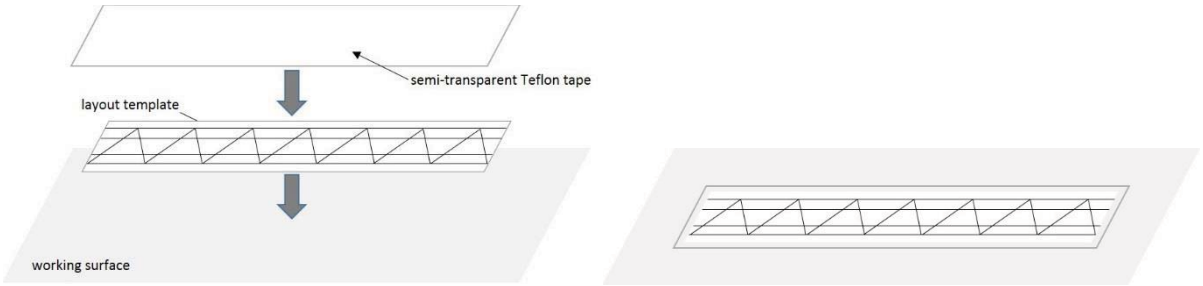

a) b)

Figure 7: a) construction of layout template; b) layout template final form

An illustration of the FO sensing fibers secured to a section of mesh positioned over a section of the lay-out template is shown in figure 8, in which the fiber is represented by the thick gray line.

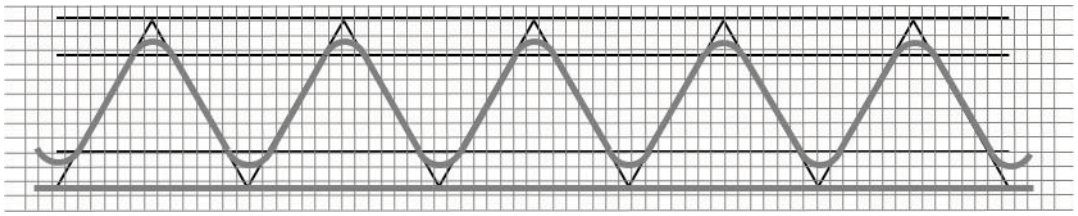

Figure 8: fiber on mesh substrate over layout template

The portions of FO cable forming the *B* and *C* sections of the rosettes were secured in straight sections between the guidelines running through the interiors of the delta templates. The actual positioning and securing of two FO sensing cables into 196 FO rosettes onto the mesh substrate was accomplished one fiber at a time. A pay-out/take-up spooling arrangement was used to unspool the mesh substrate and a FO sensing cable from two separate spools at one end of the layout template and spool up the mesh/FO configuration onto a single spool at the other end. The layout template was a little over eight rosettes in length, so only eight rosette sections were positioned at a time onto the mesh substrate. For each group of eight rosettes, a section of mesh substrate was unspooled and temporarily taped to the working surface over the layout template, after which, the necessary length of FO sensing cable needed for each section of eight rosettes was unspooled, positioned, and spot-bonded. After securing the FO cable to the mesh, the mesh/fiber combination was spooled opposite of the pay-out spools and the process would repeat. Figure 9 shows a picture of the pay-out spools, the take-up spool, and the layout template on the working surface.

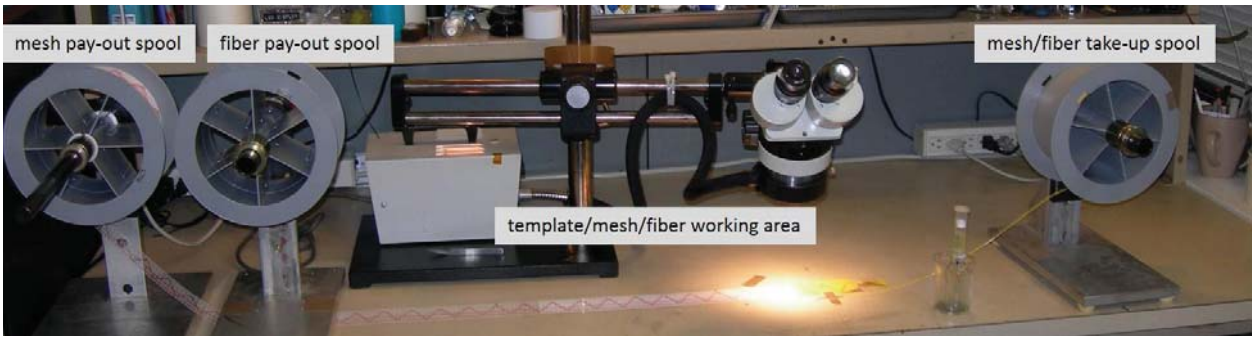

Figure 9: rosette assembly configuration

The interrogation system used in the testing had a physical limit of 40’ of sensing length per channel. Because a 40’ length of sensing fiber was not long enough to configure the entirety of the 196 rosette *B* and *C* components and because the fiber forming the rosette *A* components had several feet of unused sensing length after positioning, the fiber forming the *A* components was routed back along the mesh substrate to complete the *B* and *C* components of the remaining rosettes. In the final configuration, one fiber formed the *B* and *C* components of sensors 1 through 161 and the *B* component of sensor 162, and the other fiber formed all of the *A* components, the *C* component of sensor 162, and the *B* and *C* components of sensors 163 through 196. This configuration is diagrammed in the next section.

Substrate/Fiber Construct Installation

The substrate/fiber construct was laid out in its entirety and spot-bonded to the test article using UV-cured adhesive. It was positioned such that the fiber was in direct contact with the measurement surface. Shown in figure 10 is the layout of the final configuration on the outside of the upper section of the forward bulkhead along with exploded views of the start of the rosette pattern, the two areas of discontinuance around fasteners, the exit of the two fibers after forming the *B* and *C* components of rosette 162, and the wrap-back of the *A* component fiber to provide the *B* and *C* components of rosettes 163 through 196.

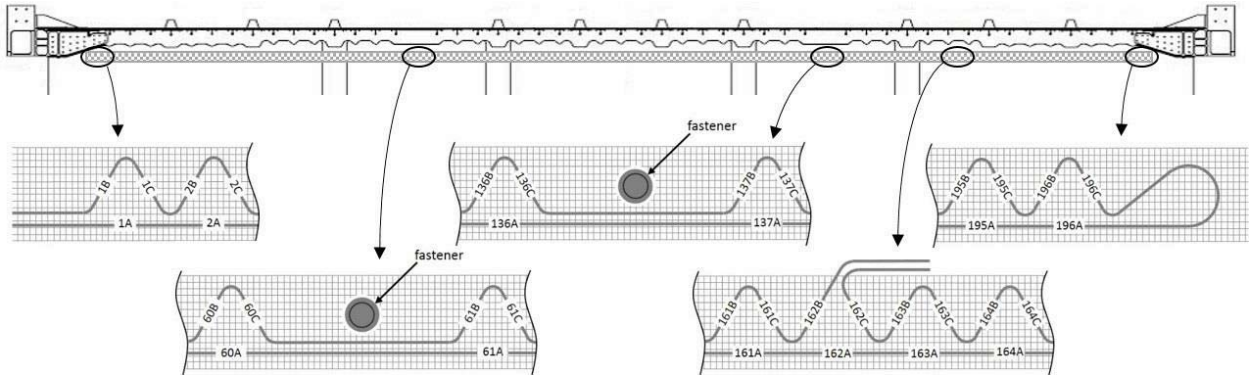

Figure 10: FO rosette configuration after installation

The substrate/fiber construct was bonded permanently in place using Hysol EA9394, a two-part, low-viscosity adhesive. With the area masked off, the adhesive was worked in through the mesh, ensuring full contact with the fibers and the measurement surface. A section of substrate/fiber construct during permanent adhesive application is shown in figure 11.

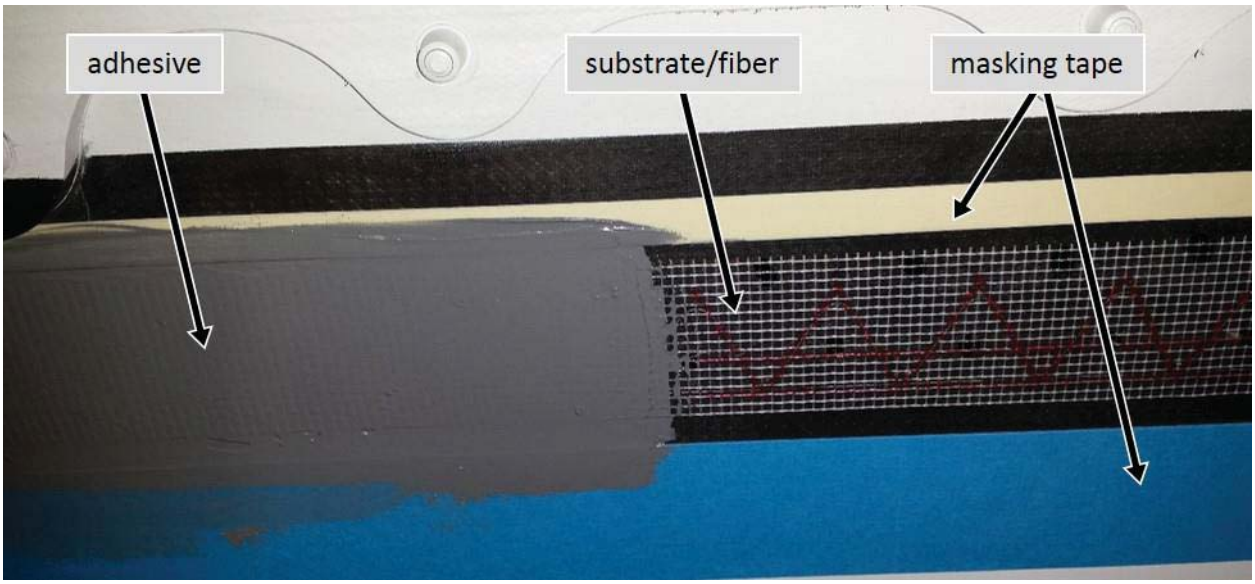

Figure 11: FO rosette permanent adhesive application

In figure 11, although difficult to distinguish, the two fibers are positioned between the mesh substrate and the test surface beneath the delta patterns marked in red on the substrate. The red line running through the interior of delta patterns was the reference line marking the center of the delta patterns. This line was used to properly locate the position of the rosettes in relation to the crown flange as according to the specification of figure 4. To minimize excess adhesive and to give an overall clean appearance, masking tape was used at the edges of the substrate/fiber construct during adhesive application. The masking tape was removed prior to adhesive curing, as any attempt to remove it after curing would be unsuccessful due to the thickness of the adhesive layer.

Measurements

Two channels of the OFDR interrogator were used to measure strain in the two individual sensing fibers used to construct the FO rosettes. Because OFDR systems distinguish measurements via their locations along the fibers, it was necessary to determine the exact location of the *A*, *B*, and *C* rosette components in their respective channel sensing space. Upon layout of the substrate/fiber construct, the locations of rosettes 1, 60, 61, 136, 137, 162, and 196 were marked on the test article, indicating the locations of the first and last rosettes in each of the three consecutively configured sections as well as the rosette where the two fibers came together to make up the components of the 162nd rosette . Because the rosette pattern was accurately repeated, determining the locations of the above listed rosettes in the sensing space of the OFDR would allow for the determination of all rosette components via simple math. To locate a component in the sensing space of the OFDR, a high-power visible light source was used to thermally excite the various rosette components while an operator observed the change in strain. As an example of this process, consider the localization of the *B* components of rosettes 1 through 60. The light source was positioned to illuminate the *B* component of rosette 1 while an operator observed the strain measurements of channel 1. The increase in strain due to temperature increase was observed to be centered at index 15.75 in the strain vs. length output of the interrogator. Note that while the “index” of the data technically has some unspecified unit of length, the conversion of index to precise length along the x-axis has not been made and is not necessary. Next the light source was positioned to illuminate the *B* component of rosette 60, upon which the strain increase due to temperature was observed to be centered at index 333. The locations of the *B* components of rosettes 2 through 59 were found using ((333-15.75)/59)x(rosette number -1) + 15.75. This process was used similarly in the localization of every rosette component of the two fibers. With all rosette components indexed in the

OFDR output, the rosette measurements were processed into and displayed as principal strain and principal direction according to common practice:

$$\varepsilon_{\max,\min} = \frac{\varepsilon_A + \varepsilon_B + \varepsilon_A}{3} \pm \frac{\sqrt{2}}{3}\sqrt{(\varepsilon_A - \varepsilon_B)^2 + (\varepsilon_B - \varepsilon_C)^2 + (\varepsilon_C - \varepsilon_A)^2} \tag{2}$$

$$\phi = \tfrac{1}{2}\tan^{-1}\left(\frac{\sqrt{3}(\varepsilon_C - \varepsilon_B)}{2\varepsilon_A - \varepsilon_B - \varepsilon_C}\right) \tag{3}$$

As an example of a typical measurement result, shown in figure 12 is the FO rosette minimum principal strain measurement (on top), the finite element model (FEM) minimum principal strain prediction for the entire forward bulkhead (middle), and minimum principal strains as measured using a video image correlation (VIC) system for a section of the aft bulkhead (bottom) for an up-bending 238.5 kip load case. For qualitative comparison, the three data presentations in figure 12 are horizontally aligned. The horizontal dashed black line crossing the upper bays of the FEM data represents the location of the FO rosette center reference line on the foreward bulkhead. Of note in the FO data is how some of the skin bays exhibited buckling that is out-of-phase with the FEM prediction. Eventhough the VIC measurements of figure 12 are taken on the aft bulkhead and the FO and FEM data are for the foreward bulkhead, the VIC data demonstrates how the actual strain and buckling behavior of the structure can differ from the predicted behaivor. The difference is acceptable in that each skin bay has more than one stable post-buckled equilibria and which one is actually triggered depends on many factors, some of which are not reflected in the finite element model (such as manufacturing geometry imperfections or residual stresses stemming from the assembly process). The FO data is in good qualitative agreement with the FEM predictions as the number of the pseudo-sine extrema per individual skin bay between consecutive frames and stringers is accurately captured. Additionally, the FO data shows good agreement with similar VIC measurements near the crown taken from the aft bulkhead. At least a portion of the disagreement between the FO rosette measurements and the VIC measurements is a result of each FO rosette measuring the average strain over a 1.5” triangular area whereas each VIC measurement point represents an average strain over a much smaller area. There were no VIC measurements nor traditional resistive-type strain guages in the vicinity of the FO rosettes locations to which to make quantitative comparison.

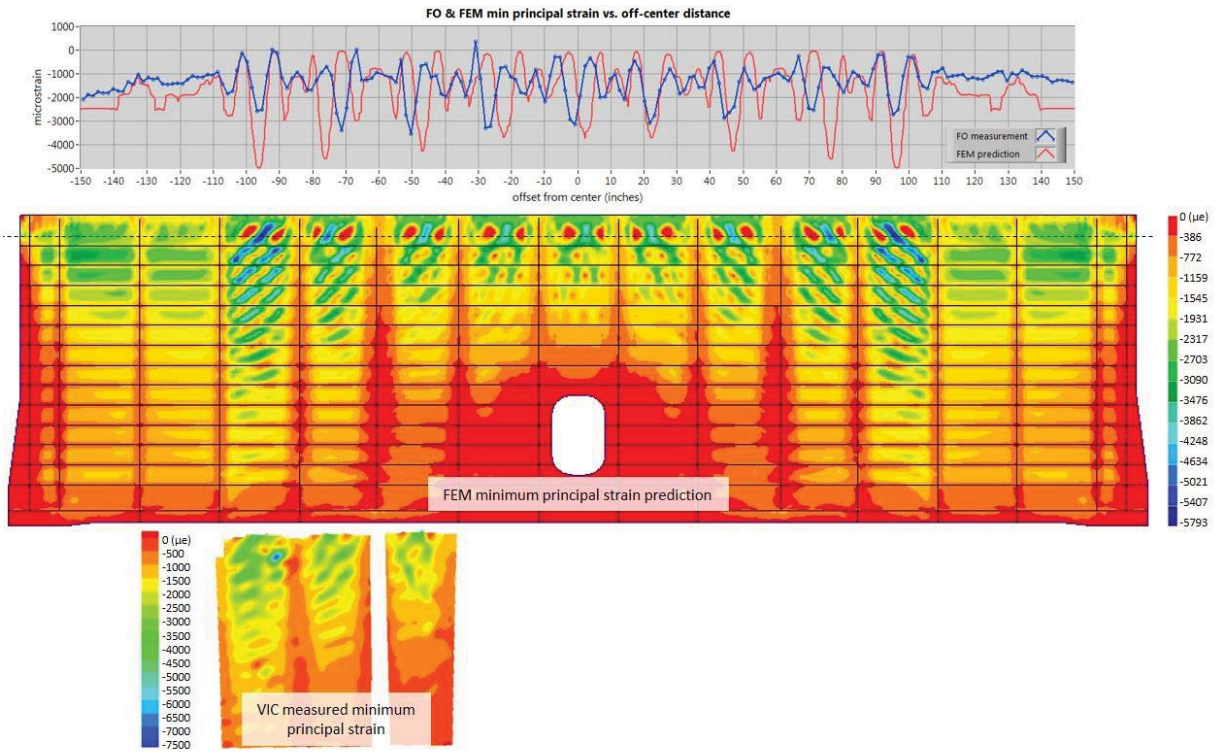

Figure 12: typcial FO rosette results

Test Data

FO rosette strain data was recorded throughout all phases of testing; however, only FO rosette strain data from the higher load and pressure test cases in the pristine condition, the damaged condition, and the final failure condition is included in this paper. A saw cut was made across the center of the crown panel of the structure to significantly weaken the test article prior to the final failure test. Each phase of testing had specific load and pressure goals and in most cases, those specific loads and pressures were held constant for a minimum of 3 seconds. At each hold point as many FO scans as possible were used to produce average FO measurement values. Because there was no hold-point during the final load-to-failure test, the scans taken just prior to total failure were used to form the average FO measurements at the failure load. The FO rosette data for the load and pressure points listed in Table 1 are plotted in *appendix b*.

Table 1: load and pressure hold points at which FO data was averaged

Load (kips)	Pressure (psi)	# FO scans averaged	Structural state
-95.4	0.0	57	pristine
-95.4	13.8	50	pristine
0.0	18.4	150	pristine
238.5	0.0	56	pristine
238.5	13.8	42	pristine
-95.4	0.0	111	impact-damaged

-95.4	13.8	74	impact-damaged
0.0	18.4	52	impact-damaged
238.5	0.0	30	impact-damaged
238.5	13.8	490	impact-damaged
262.4	13.8	156	impact-damaged
262.4	0.0	29	impact-damaged
270.2	0.0	50	saw-cut

Results and Conclusions

Because there was no co-located surface strain measurement system to which to compare the FO rosette data, there is no quantitative error analysis presented here. The patterns in the FO rosette data, however, are consistent with the expected reaction of the test article to the various loads and pressures given the stiffener locations on the interior of the bulkhead structure to the which the FO rosette gauges were applied. Possible sources of error are the general error of the interrogation system and the possibility that some of the rosette component measurements may have been affected by the inclusion of curved sections of fiber. Because the precise section of fiber associated with each rosette component could not be specifically processed within the interrogator, interpolation between the measurements of two adjacent half-inch long fiber sections was used to formulate the measurements at each component location. This simple form of interpolation opens up the possibility that one of the half-inch long sections of fiber may have included fiber that was not purely in the component axis of interest and lying at least partially along a curved portion of the fiber layout. Augmenting the interrogator software to process specific fiber sections would eliminate this possible source of error.

Improvements can be implemented concerning the process of constructing the mesh/fiber construct. As an example, the process could include a machine-assisted method to improve layout accuracy and lessen fiber layout time. The drywall joint tape seemed to function properly as a securing mechanism for the layout pattern and as a non-effecting component after permanent bonding, however further trials will be necessary to affirm that assumption. Further trials are absolutely necessary with the inclusion of a third party measurement to which to compare FO rosette data for the purpose of quantifying reliability and accuracy of the method and measurements.

References

1. Dawn Jegley, Marshall Rouse, Adam Przekop, and Andrew Lovejoy, “The Behavior of a Stitched Composite Large-Scale Multi-Bay Pressure Box,” NASA TM 2015-218972, December 2015.

2. Othonos, Andreas; Kalli, Kyriacos. Fiber Bragg gratings : fundamentals and applications in telecommunications and sensing. 1999 Artech House, Inc. Norwood, MA.

3. Handbook of Optical Sensors,Edited by Jose Luis Santos and Faramarz Farahi,CRC Press 2014

Appendix

Appendix a: rosette layout template drawing

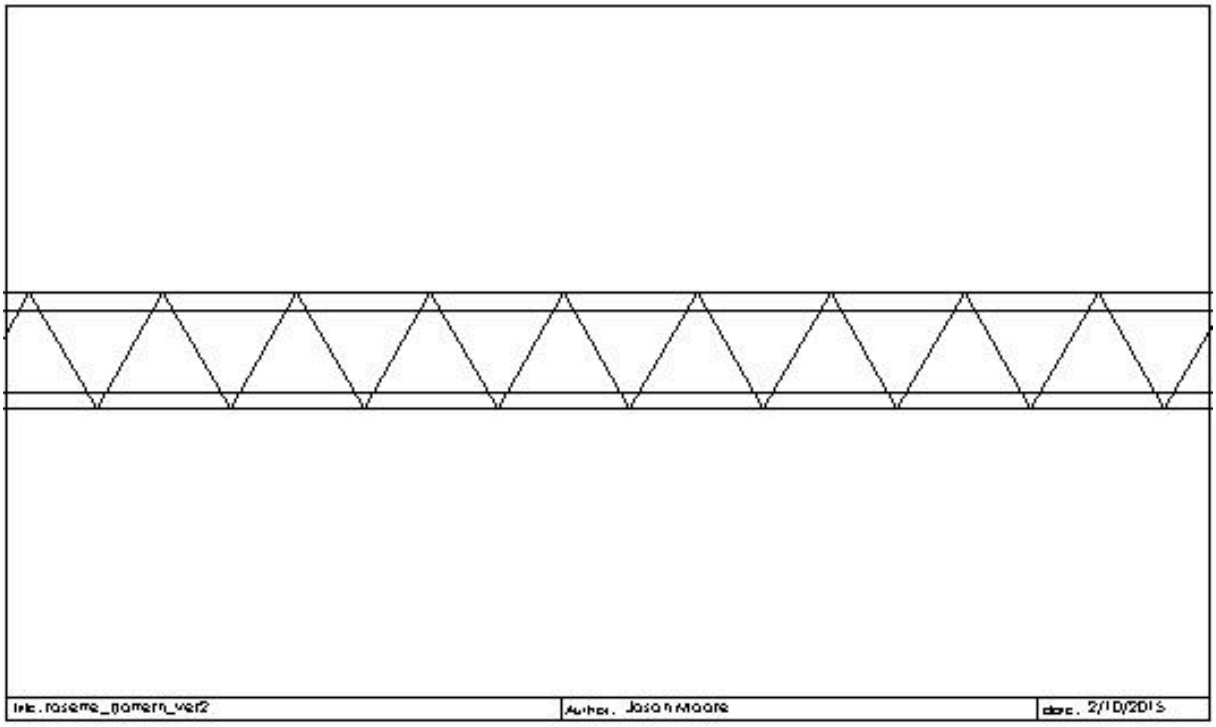

Appenix b: Fiber Optic Rosette Measurements of Table 1 Test Points

-95.4 kips, 0.0 psi, pristine

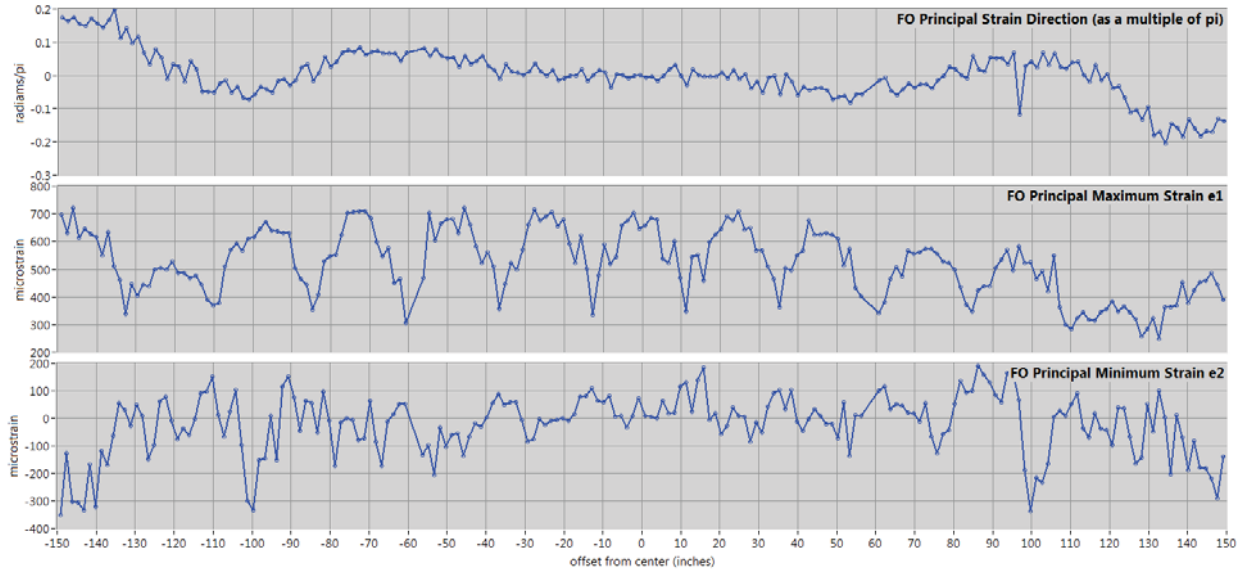

-95.4 kips, 13.8 psi, pristine

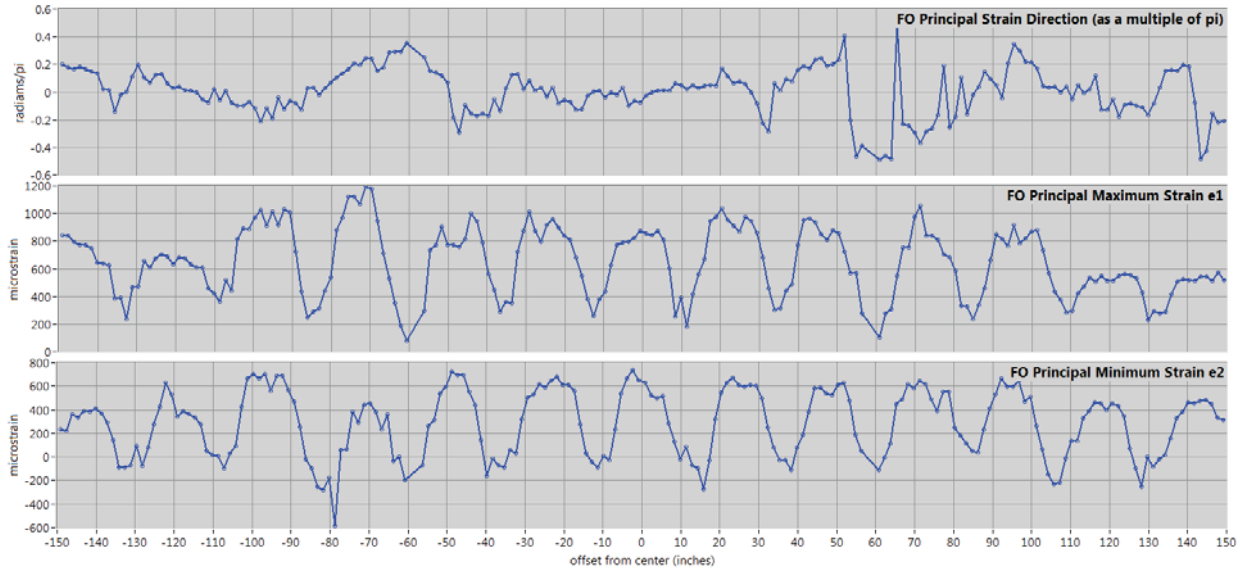

0.0 kips, 18.4 psi, pristine

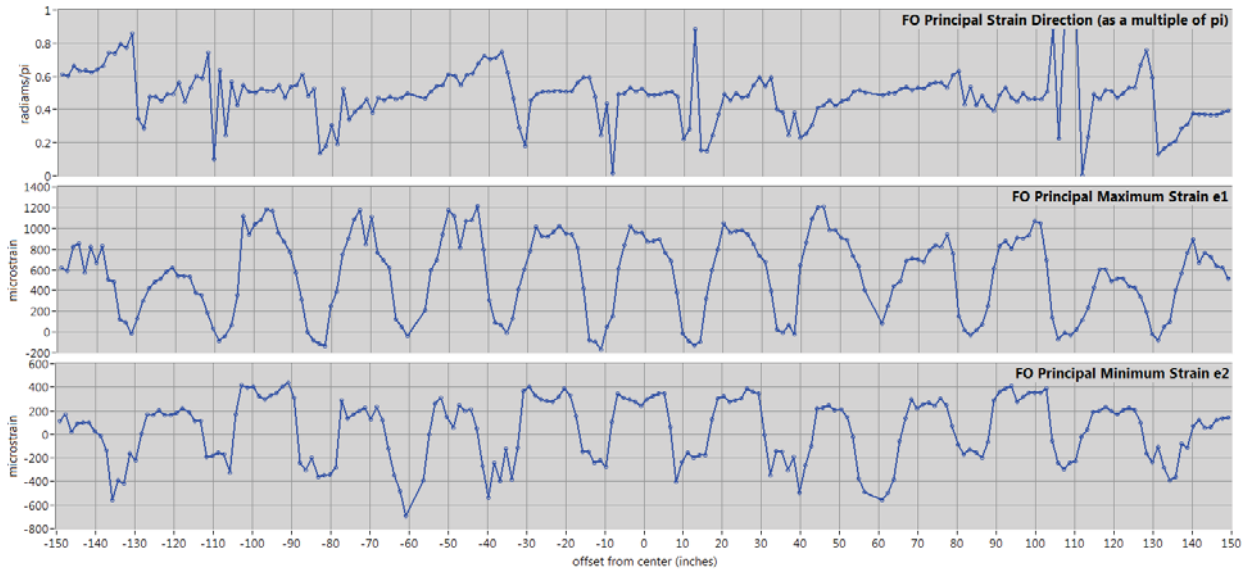

238.5 kips, 0.0 psi, pristine

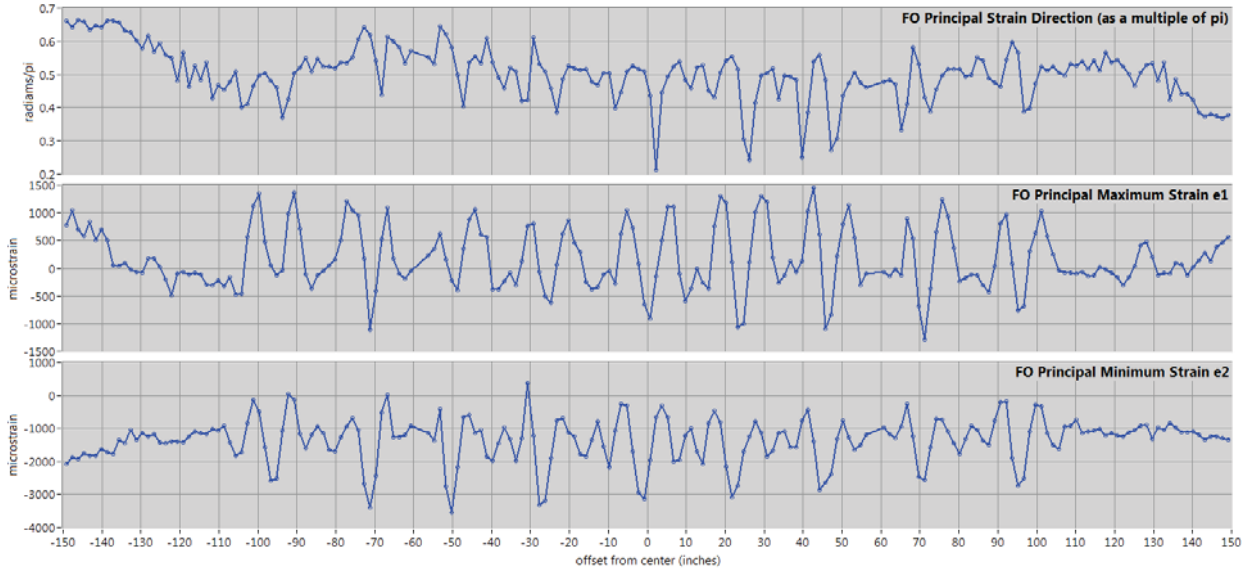

238.5 kips, 13.8 psi, pristine

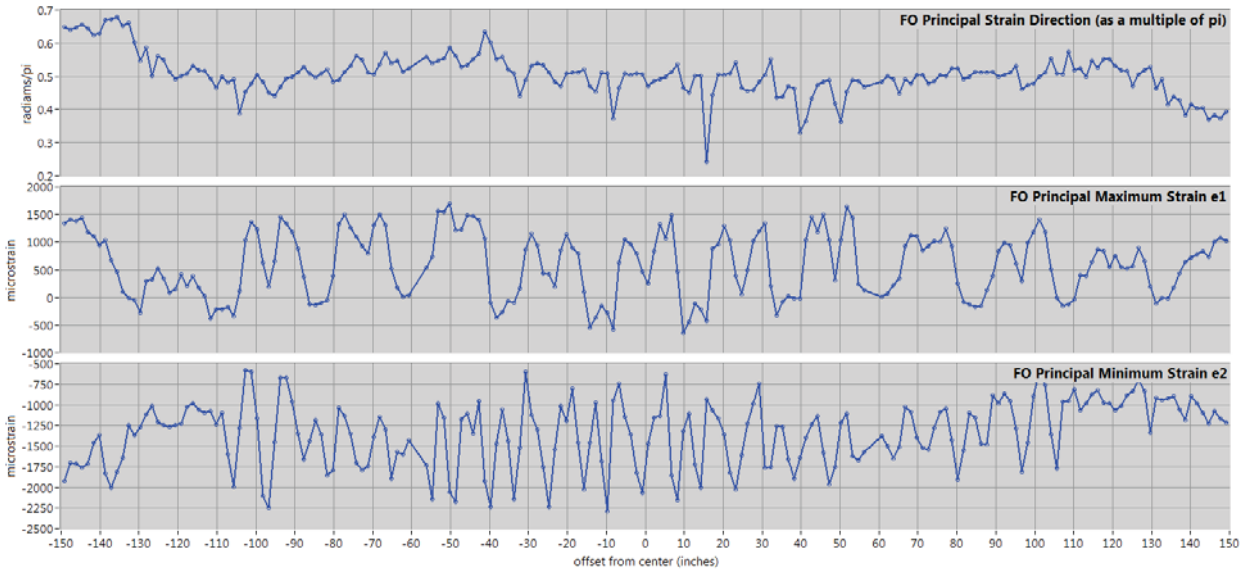

-95.4 kips, 0.0 psi, impact-damaged

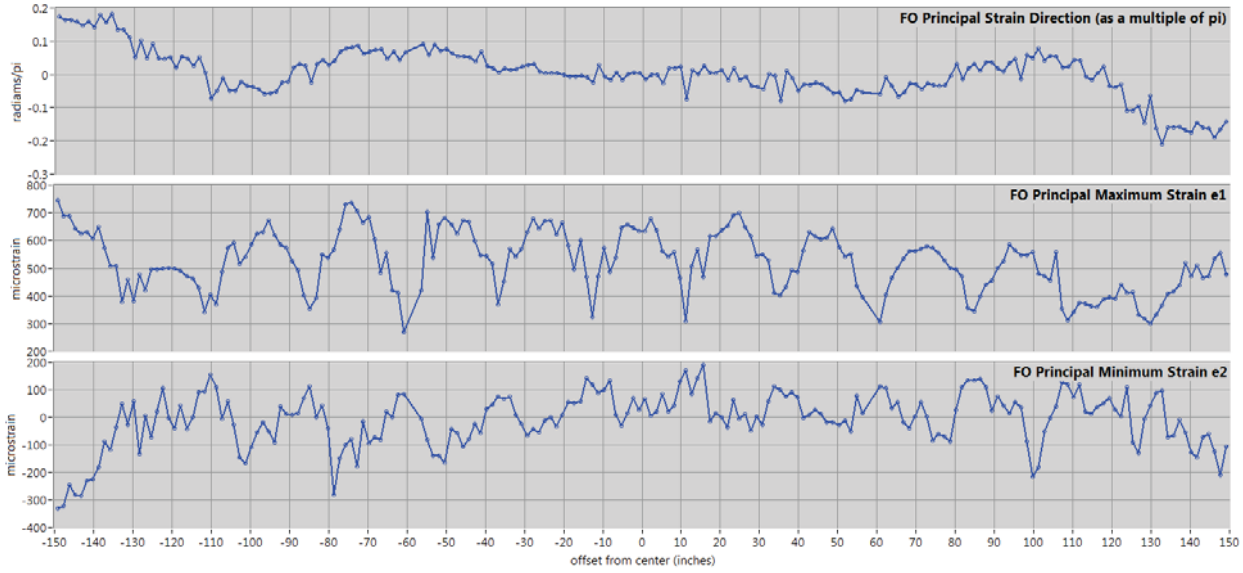

-95.4 kips, 13.8 psi, impact-damaged

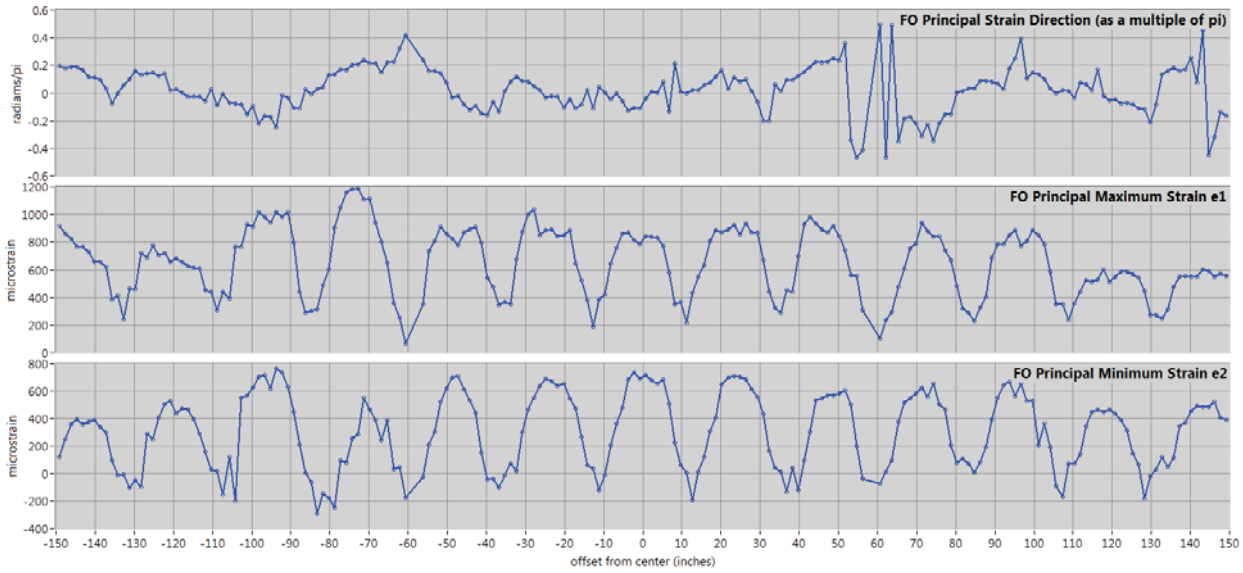

0.0 kips, 18.4 psi, impact-damaged

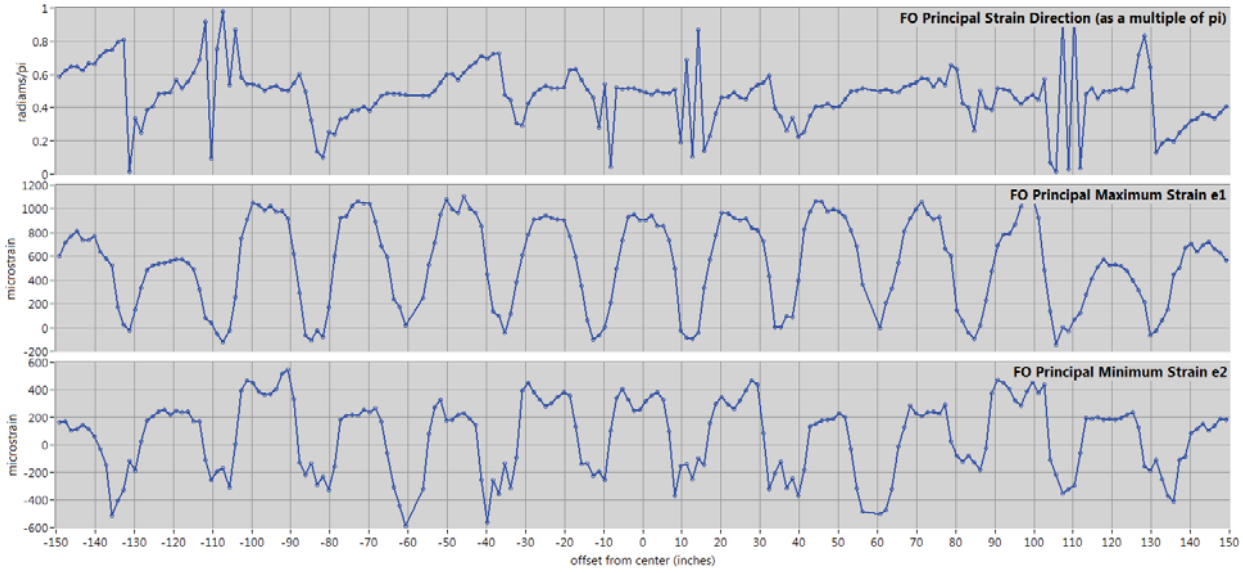

238.5 kips, 0.0 psi, impact-damaged

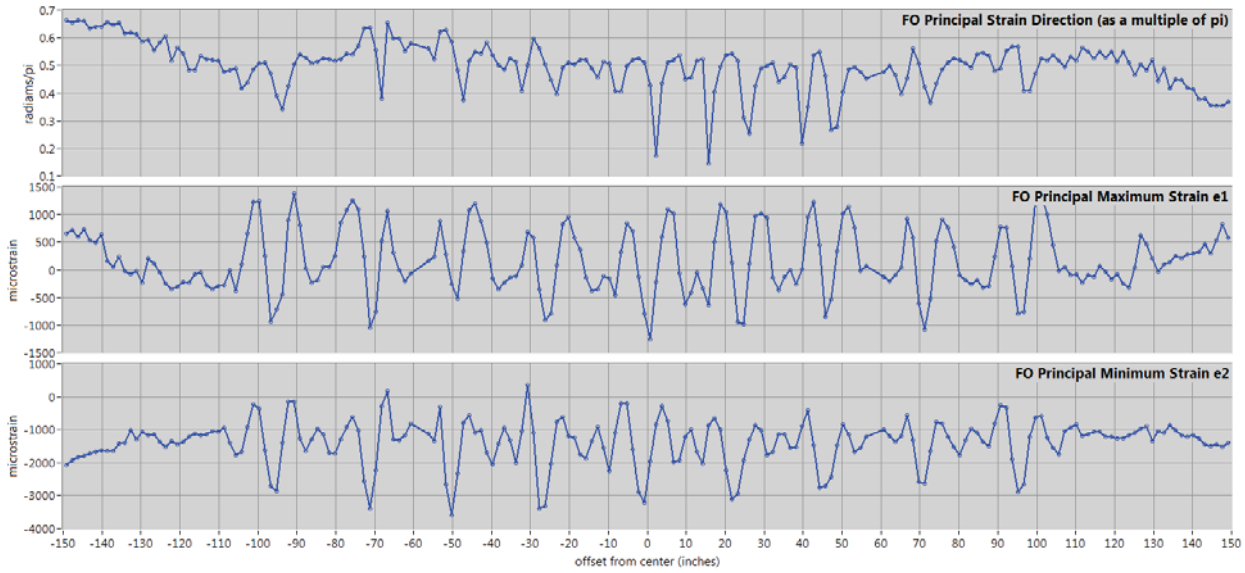

238.5 kips, 13.8 psi, impact-damaged

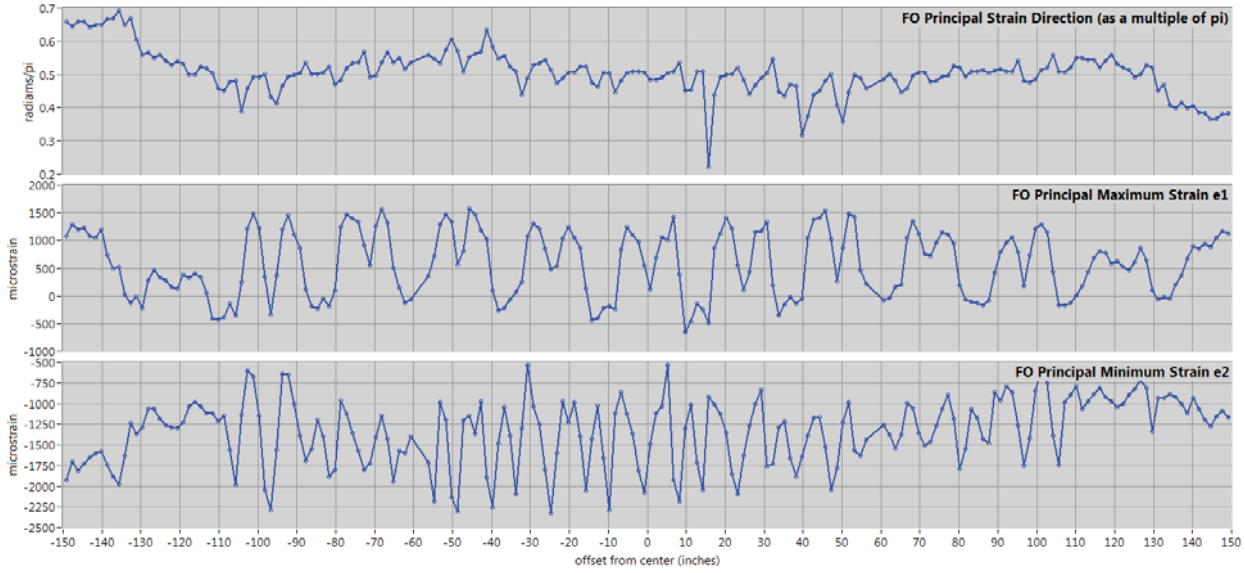

262.4 kips, 13.8 psi, impact-damaged

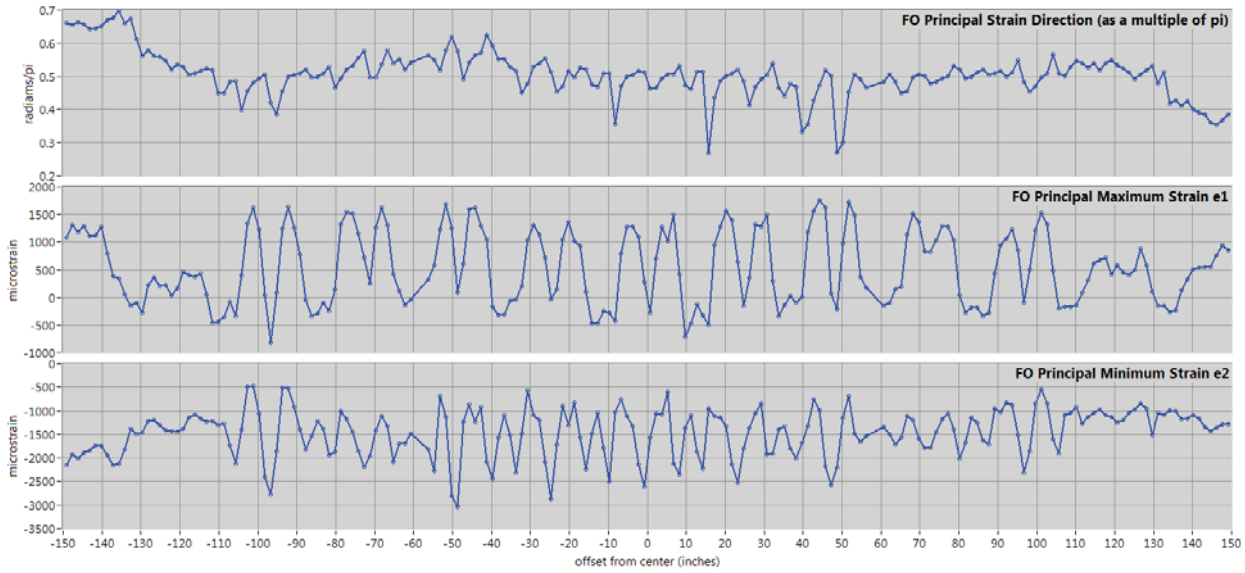

262.4 kips, 0.0 psi, impact-damaged

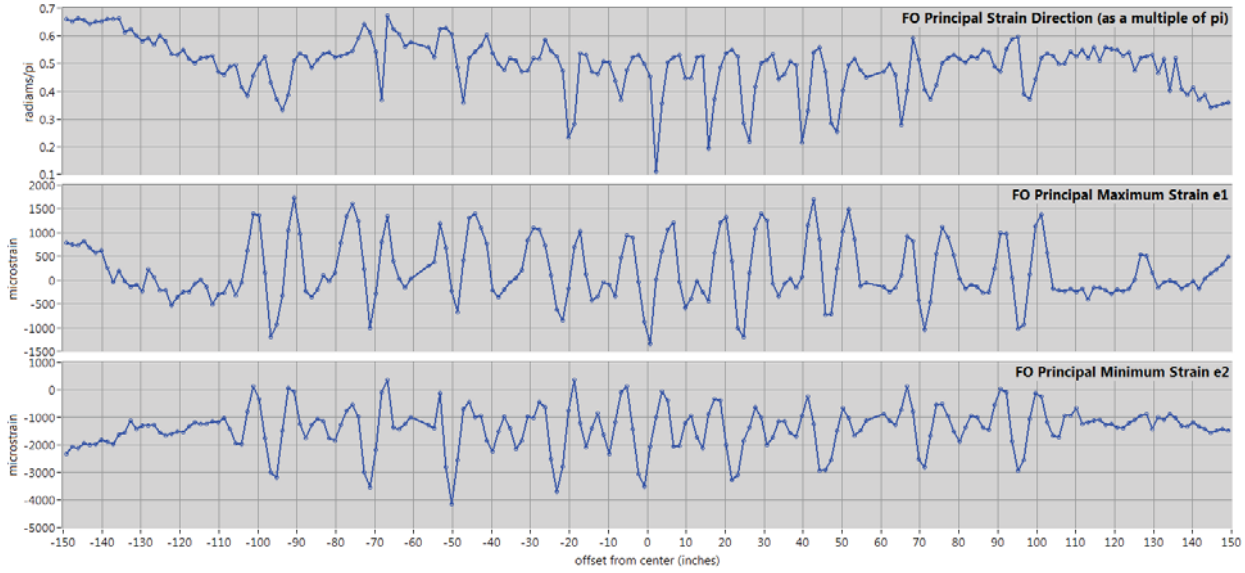

270.2 kips, 0.0 psi, saw-cut

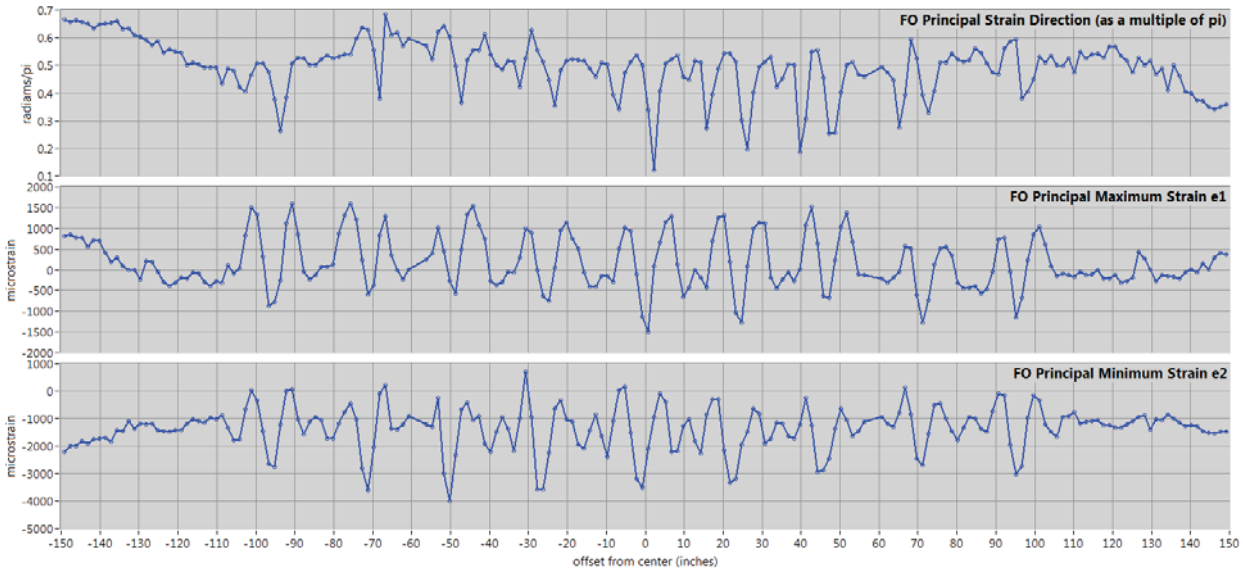

REPORT DOCUMENTATION PAGE

Form Approved
OMB No. 0704-0188

1. REPORT DATE *(DD-MM-YYYY)*	2. REPORT TYPE	3. DATES COVERED *(From - To)*
01- 12 - 2015	Technical Memorandum	

4. TITLE AND SUBTITLE

Fiber Optic Rosette Strain Gauge Development and Application on a Large-scale Composite Structure

5a. CONTRACT NUMBER

5b. GRANT NUMBER

5c. PROGRAM ELEMENT NUMBER

6. AUTHOR(S)

Moore, Jason P.; Przekop, Adam; Juarez, Peter D.; Roth, Mark C.

5d. PROJECT NUMBER

5e. TASK NUMBER

5f. WORK UNIT NUMBER

338881.02.22.07.01.01

7. PERFORMING ORGANIZATION NAME(S) AND ADDRESS(ES)

NASA Langley Research Center
Hampton, VA 23681-2199

8. PERFORMING ORGANIZATION REPORT NUMBER

L-20627

9. SPONSORING/MONITORING AGENCY NAME(S) AND ADDRESS(ES)

National Aeronautics and Space Administration
Washington, DC 20546-0001

10. SPONSOR/MONITOR'S ACRONYM(S)

NASA

11. SPONSOR/MONITOR'S REPORT NUMBER(S)

NASA-TM-2015-218970

12. DISTRIBUTION/AVAILABILITY STATEMENT

Unclassified - Unlimited
Subject Category 74
Availability: NASA STI Program (757) 864-9658

13. SUPPLEMENTARY NOTES

14. ABSTRACT

A detailed description of the construction, application, and measurement of 196 FO rosette strain gauges that measured multi-axis strain across the outside upper surface of the forward bulkhead component of a multi-bay composite fuselage test article is presented. A background of the FO strain gauge and the FO measurement system as utilized in this application is given and results for the higher load cases of the testing sequence are shown.

15. SUBJECT TERMS

Fiber Bragg Gratings; Fiber optic sensors; Fiber optics

16. SECURITY CLASSIFICATION OF:			17. LIMITATION OF ABSTRACT	18. NUMBER OF PAGES	19a. NAME OF RESPONSIBLE PERSON
a. REPORT	b. ABSTRACT	c. THIS PAGE			STI Help Desk (email: help@sti.nasa.gov)
					19b. TELEPHONE NUMBER *(Include area code)*
U	U	U	UU	24	(757) 864-9658